

# Calibration of Implied Volatility in Generalized Hull-White Model

Fangfang Zhao<sup>1</sup>, Zuoliang Xu<sup>1</sup>, Changjing Li<sup>2</sup>

<sup>1</sup>School of Information, Renmin University of China, Beijing, China

<sup>2</sup>School of Mathematical Sciences, Shandong Normal University, Jinan, China

## Email address:

wanwanf2@163.com (Fangfang Zhao), xuzl@ruc.edu.cn (Zuoliang Xu)

## To cite this article:

Fangfang Zhao, Zuoliang Xu, Changjing Li. Calibration of Implied Volatility in Generalized Hull-White Model. *Journal of Finance and Accounting*. Vol. 4, No. 2, 2016, pp. 25-32. doi: 10.11648/j.jfa.20160402.11

---

**Abstract:** This paper concerns a problem of calibrating implied volatility in generalized Hull-White model from the market prices of zero-coupon bonds. By using the regularization method, we establish the existence and stability of the optimal solution, and give the necessary condition that the solution satisfies. Finally numerical results show that the method is stable and effective.

**Keywords:** Calibration, Implied Volatility, Generalized Hull-White Model, Regularization

---

## 1. Introduction

Interest rate is one of the most basic economic variables in financial market. In finance, the solutions to many problems, such as the design, the pricing and innovation of financial products, have to be based on the study of the term structure of interest rate. Research of the term structure and the dynamic risk management of interest rates directly relates to the financial market, especially the bond market's stability and prosperity. In recent years, along with the rapid development and expand of the bond market, many new types of bonds and other interest rate derivatives emerge constantly, the research on term structure of interest rate becomes more important. In finance, how to establish the interest rate model or characteristic the dynamic changes of the term structure effectively, thus to predict the future changes in interest rates scientifically, is difficult and meaningful. So far, a lot of interest rate models have been proposed and widely used. In general, assuming the short term interest rate as  $r$ , we use the following stochastic differential equation to establish the interest rate model

$$dr = \mu(r, t)dt + \sigma(r, t)dZ(t), \quad (1)$$

Where  $\mu(r, t)$  is the drift term and denotes the instantaneous expectation of the interest rate changes,  $\sigma(r, t)$  is called the volatility or diffusion term which denotes the instantaneous variance of the interest rate changes,  $Z(t)$  denotes a standard Wiener process.

Different interest rate models have the different drift or

volatility terms, in which the most widely used interest rate model is the single factor model, such as Vasicek model, CIR model, Hull-White model(1990), CEV model and Hull-White model (1994) [1]-[5]. In [6], Hull and White give the generalized Hull-White model in which some function of the short-rate obeys a Gaussian diffusion process of the following form

$$df(r) = (\theta(t) - a(t)f(r))dt + \sigma(t)dZ(t). \quad (2)$$

where  $\theta(t), a(t)$  and  $\sigma(t)$  are deterministic functions of  $t$ ,  $f(r)$  is a function of  $r$ . The generalized Hull-White model contains many popular term structure models as special cases. In this paper, we consider the case that  $a$  is a constant and  $f(r) = r$ .

Since parameters in the interest rate model can not be directly observed, in order to truly describe the market data information, thus to better price the interest rate derivatives and risk measurement, it is necessary to solve the inverse problem of calibrating parameters that are used in the term structure model. Much research has been done on the inverse problem to reconstruct parameters from market prices [7]-[12]. At present, there are many methods to solve this kind of problems, such as regularization method, maximum likelihood method, full Bayesian method and optimization method [13]-[15]. In [16], Tang and Chen develop expansions for the bias and variance of parameter estimators for Vasicek and CIR processes, which helps to understand why the drift parameters are more difficult to estimate than the diffusion

parameter, and then they study the first order approximate maximum likelihood estimator for linear drift processes. A parametric bootstrap procedure is proposed to correct bias for general diffusion processes with a theoretical justification. In [17], Rainer gives the general structure of optimization in the context of calibration of stochastic models for interest rate derivatives. Based on the relevant market data, a novel numerical algorithm for the optimization of parameters in interest rate models is presented. In [18], Rodrigo and Mamon propose a new method to calibrate the Vasicek and CIR models by defining an appropriate generating function and deriving recursive relations between the derivatives of the generating function and the bond prices. The parameters of the models are then recovered by solving a system of linearly independent equations arising from the recursive relations.

In all of the above papers, zero-coupon prices, yield rate curves, or forward rate curves are treated as inputs. In this paper, based on [18], with the regularization theory, we propose a new regularization method to calibrate the implied volatility of interest rate in generalized Hull-White model from the market prices of zero-coupon bond. By using the regularization method, we establish the existence and stability of the solution, and give the necessary condition the solution satisfies. Finally numerical results show that the method is feasible.

The outline of this paper is as follows. In section 2, based on the generalized Hull-White model, we formulate the calibration problem. In Section 3, we address the regularization method to transform the calibration problem into the regularization problem and give the main results in this paper. In section 4, we present the results of our numerical experiments. In section 5, some concluding remarks are given.

## 2. Formulation of the Calibration Problem

In this section, based on the generalized Hull-White model, the calibration problem of implied volatility is formulated.

In this paper, we consider the following generalized Hull-White model. Under the risk-neutral measure, suppose that the behavior of short-term interest rate  $r = r_t = r(t)$  is modeled by the following stochastic differential equation

$$dr_t = (\theta(t) - ar)dt + \sigma(t)dZ(t), \quad (3)$$

where  $a$  is a constant speed of mean reversion,  $Z(t)$  denotes a standard Wiener process,  $\theta(t), \sigma(t)$  are deterministic functions of time  $t$ , and  $\theta(t)/a$  represents the mean-reverting level.

Denote the price of a zero-coupon bond at time  $t$  with maturity  $T$  by  $P(t, T)$  of which the face value is one unit. Based on the above model, it has a risk-neutral valuation representation

$$P = \mathbb{E}(e^{-\int_t^T r(s)ds} | r(t)), \quad (4)$$

where  $\mathbb{E}(\cdot)$  denotes the expectation operator. Applying the general method for derivative security pricing [3], we get the partial differential equation for a zero-coupon bond in the form

$$\frac{\partial P}{\partial t} + \frac{\sigma^2(t)}{2} \frac{\partial^2 P}{\partial r^2} + (\theta(t) - ar) \frac{\partial P}{\partial r} - rP = 0. \quad (5)$$

The final condition is given by

$$P(T, T) = 1. \quad (6)$$

It is known that the solution of the equations (5)-(6) has an exponential affine form [19]

$$P(t, T) = \exp(A(t, T) - r_t B(t, T)). \quad (7)$$

Substituting (7) into (5) gives

$$A'(t, T) + \frac{\sigma^2(t)}{2} B^2(t, T) - \theta(t)B(t, T) = 0, \quad A(T, T) = 0, \quad (8)$$

$$B'(t, T) - aB(t, T) + 1 = 0, \quad B(T, T) = 0. \quad (9)$$

Solving the above ordinary differential equations, we obtain

$$A(t, T) = \int_t^T \left( \frac{\sigma^2(s)}{2} B^2(s, T) - \theta(s)B(s, T) \right) ds, \quad (10)$$

$$B(t, T) = \frac{1 - e^{-a(T-t)}}{a}. \quad (11)$$

Given the market prices of zero-coupon bond  $P^*(0, T)$  with different maturities  $T$ , we consider the following calibration problem.

Calibration problem. Determine the implied volatility function  $\sigma(t)$  such that the solution of (5)-(6) at initial time  $t = 0$  satisfies

$$P(0, T) \doteq P^*(0, T), \quad T \in [0, \hat{T}], \quad (12)$$

where  $\hat{T}$  is the largest maturity of zero-coupon bond.

Here the crucial step is how to define  $\doteq$  in (12), so that the theoretical price fits the empirical price as well as possible. The common definitions are

$$P(0, T) = P^*(0, T), \quad (13)$$

$$\log P(0, T) = \log P^*(0, T), \quad (14)$$

for all  $T \in [0, \hat{T}]$  or the mean square error

$$\int_0^{\hat{T}} [P(0, u) - P^*(0, u)]^2 du. \quad (15)$$

is minimized for each  $T \in [0, \hat{T}]$ .

In this paper, we define  $\doteq$  as

$$\int_0^{\hat{T}} u^n \log P(0, u) du = \int_0^{\hat{T}} u^n \log P^*(0, u) du, \quad (16)$$

where  $n$  is a non-negative integer [18]. In other words, it can be interpreted as that all of the moments of  $\log P(0, \cdot)$  and  $\log P^*(0, \cdot)$  are equal.

### 3. Regularization Method

In this section, applying the regularization method to calibrate the implied volatility, we transform the calibration problem to the regularization problem and obtain the existence and stability of the solution, as well as the necessary condition that the solution satisfies.

#### 3.1. Calibration Problem Transformation

Firstly, from the equation (7), we get

$$\log P(0, T) = A(0, T) - r_0 B(0, T), \tag{17}$$

and then have

$$\int_0^T u^n A(0, u) du - r_0 \int_0^T u^n B(0, u) du = \int_0^T u^n \log P^*(0, u) du, \tag{18}$$

From the equation (10)-(11),

$$A(0, T) = \int_0^T \left( \frac{\sigma^2(s)}{2} B^2(s, T) - \theta(s) B(s, T) \right) ds, \tag{19}$$

$$B(0, T) = \frac{1 - e^{-aT}}{a}, \tag{20}$$

Thus

$$\begin{aligned} \int_0^T u^n A(0, u) du &= \int_0^T u^n \int_0^u \left( \frac{\sigma^2(s)}{2} B^2(s, u) - \theta(s) B(s, u) \right) ds du \\ &= \int_0^T \sigma^2(s) \int_s^T \frac{u^n B^2(s, u)}{2} du ds - \int_0^T u^n \int_0^u \theta(s) B(s, u) ds du \\ &= \int_0^T \rho(s) L_n(s, T) ds - \int_0^T u^n \int_0^u \theta(s) B(s, u) ds du, \end{aligned}$$

where

$$\rho(s) = \sigma^2(s), \quad L_n(s, T) = \int_s^T \frac{u^n (1 - e^{-a(u-s)})^2}{2a^2} du. \tag{21}$$

In the remainder of this paper, we take the calibration of volatility  $\sigma(t)$  equivalent to that of  $\rho(t)$ . Inserting the above equation into the equation (18) and rearranging it, we have

$$\int_0^T \rho(s) L_n(s, T) ds = g_n(T), n = 0, 1, \dots, \tag{22}$$

where

$$\begin{aligned} g_n(T) &= \int_0^T u^n \log P^*(0, u) du + r_0 \int_0^T u^n B(0, u) du \\ &\quad + \int_0^T u^n \int_0^u \theta(s) B(s, u) ds du. \end{aligned} \tag{23}$$

Define operators  $K_n$  as follows

$$K_n \rho := \int_0^T \rho(s) L_n(s, T) ds, \tag{24}$$

then we have

$$K_n \rho = g_n(T). \tag{25}$$

The equation (25) is a Fredholm integral equation of the first kind and is an ill-posed problem under noisy propagation. Thus, the calibration problem is transformed into the following regularization problem which lies in minimization of the functional

$$\min_{\rho \in \Omega} J_\lambda(\rho) := \sum_{n=0}^k \frac{1}{2} \|K_n \rho - g_n(T)\|^2 + \frac{1}{2} \lambda_1 \|\rho\|^2 + \frac{1}{2} \lambda_2 \|\rho'\|^2, \tag{26}$$

where  $\lambda = \{(\lambda_1, \lambda_2) \mid \lambda_1, \lambda_2 > 0\}$  is the so-called regularization parameters,  $k$  is a limited nonnegative integer.  $\|\cdot\|$  denotes the Euclidean  $L^2$ -norm. Here we define  $\Omega$  as

$$\Omega = \{\rho(t) \in H^1([0, \hat{T}]) \mid \rho'(0) = 0, \rho'(\hat{T}) = 0\}. \tag{27}$$

which implies the volatility at the initial and long time is a constant.

#### 3.2. Main Results

Theorem 1 (Existence) There exists at least one minimal element  $\bar{\rho} \in \Omega$ , such that

$$J_\lambda(\bar{\rho}) = \min_{\rho \in \Omega} J_\lambda(\rho). \tag{28}$$

Proof. Suppose  $\rho_m$  is a minimizing sequence, we have

$$\inf_{\rho \in \Omega} J_\lambda(\rho) \leq J_\lambda(\rho_m) \leq \inf_{\rho \in \Omega} J_\lambda(\rho) + \frac{1}{m}, \tag{29}$$

As  $\|J(\rho_m)\| \leq C$ , it is obviously to get  $(\rho_m, K_n \rho_m)$  are bounded. Take a weak convergence subsequence arbitrarily and denote as  $(\rho_m, K_n \rho_m)$  still for convenience.

Thus

$$\rho_m \rightarrow \bar{\rho}, K_n \rho_m \rightarrow g_n. \tag{30}$$

Form the property of  $K_n$ , we can get  $\bar{\rho} \in \Omega, K_n \bar{\rho} = g_n$ .

Hence as the results of Lebesgue control convergence theorem and the weakly lower semi-continuity of  $L^2$ -norm, we obtain

$$J_\lambda(\bar{\rho}) \leq \liminf_{n \rightarrow \infty} J_\lambda(\rho_n) = \min_{\rho \in \Omega} J_\lambda(\rho). \tag{31}$$

Therefore  $J_\lambda(\bar{\rho}) = \min_{\rho \in \Omega} J_\lambda(\rho)$ , which means  $\bar{\rho}$  is one of the solutions of the regularization problem (26).

Theorem 2 (Stability) Suppose  $g_{n,\delta}(T)$  are data with perturbation and

$$\|g_{n,\delta}(T) - g_n(T)\| \leq \delta. \tag{32}$$

In addition, we assume  $\rho_{\lambda,\delta}(t), \rho_\lambda(t)$  are the solutions of the regularization problem (26) respectively corresponding to  $g_{n,\delta}(T)$  and  $g_n(T)$ . Let  $e(t) = \rho_\lambda(t) - \rho_{\lambda,\delta}(t)$ , then we have

$$\|e\| \leq \frac{\sqrt{k+1}\delta}{2\sqrt{\lambda_1}}. \quad (33)$$

Proof. As  $\rho_{\lambda,\delta}(t)$  is the minimal solution of  $J_\lambda(\rho)$  corresponding to  $g_{n,\delta}(T)$ , then for  $\forall 0 \leq \alpha \leq 1$ ,  $\rho_{\lambda,\delta}(t) + \alpha e \in \Omega$ , we have

$$\frac{d}{d\alpha} J_\lambda(\rho_{\lambda,\delta}(t) + \alpha e) \Big|_{\alpha=0} = 0. \quad (34)$$

Calculating the above equation gives

$$\sum_{n=0}^k \langle K_n \rho_{\lambda,\delta} - g_{n,\delta}, K_n e \rangle + \lambda_1 \langle \rho_{\lambda,\delta}, e \rangle + \lambda_2 \langle \rho'_{\lambda,\delta}, e' \rangle = 0. \quad (35)$$

Similarly, we obtain

$$\sum_{n=0}^k \langle K_n \rho_\lambda - g_n, K_n e \rangle + \lambda_1 \langle \rho_\lambda, e \rangle + \lambda_2 \langle \rho'_\lambda, e' \rangle = 0. \quad (36)$$

Subtracting the equation (36) from (35) and using the Schwartz's inequality yields

$$\begin{aligned} & \sum_{n=0}^k \|K_n e\|^2 + \lambda_1 \|e\|^2 + \lambda_2 \|e'\|^2 \\ &= \sum_{n=0}^k \langle g_{n,\delta} - g_n, K_n e \rangle \\ &\leq \delta \sum_{n=0}^k \|K_n e\| \leq \frac{(k+1)\delta^2}{4} + \sum_{n=0}^k \|K_n e\|^2. \end{aligned} \quad (37)$$

then

$$\lambda_1 \|e\|^2 \leq \lambda_1 \|e\|^2 + \lambda_2 \|e'\|^2 \leq \frac{(k+1)\delta^2}{4}. \quad (38)$$

So we have

$$\|e\| \leq \frac{\sqrt{k+1}\delta}{2\sqrt{\lambda_1}}.$$

The above theorem shows that the solution of the regularization problem (26) is stable. In the following, we will give the necessary condition by calculating the Euler equation.

Theorem 3 (Necessary condition) Suppose  $\rho_\lambda(t)$  as the solution of the regularization problem (26), then  $\rho_\lambda(t)$  satisfies

$$\sum_{n=0}^k H_n(\rho_\lambda) + \lambda_1 \rho_\lambda - \lambda_2 \rho''_\lambda = 0, \quad (39)$$

where

$$H_n \rho_\lambda = \int_0^{\hat{T}} \tilde{L}_n(s,t) \rho_\lambda(t) dt - \int_s^{\hat{T}} g_n(T) L_n(s,T) dT, s \in [0, \hat{T}], \quad (40)$$

and

$$\tilde{L}_n(s,t) = \begin{cases} \int_s^T L_n(s,T) L_n(t,T) dT, t \in [0, s], \\ \int_t^T L_n(s,T) L_n(t,T) dT, t \in [s, \hat{T}]. \end{cases} \quad (41)$$

Proof. For  $\forall 0 \leq \alpha \leq 1$ , assume

$$\tilde{\rho}(t) = \rho_\lambda(t) + \alpha(\rho^*(t) - \rho_\lambda(t)). \quad (42)$$

Obviously, we have  $\tilde{\rho}(t) \in \Omega$  if  $\rho^*(t), \rho_\lambda(t) \in \Omega$ . By using the Fubini theorem, we get

$$\frac{dJ_\lambda(\tilde{\rho})}{d\alpha} \Big|_{\alpha=0} = 0. \quad (43)$$

Denote  $\rho^*(t) - \rho_\lambda(t) = \varphi(t)$  and integral by parts,

$$\sum_{n=0}^k \langle K_n \rho_\lambda - g_n(T), K_n \varphi \rangle + \lambda_1 \langle \rho_\lambda, \varphi \rangle - \lambda_2 \langle \rho''_\lambda, \varphi \rangle = 0. \quad (44)$$

$$\begin{aligned} & \langle K_n \rho_\lambda - g_n(T), K_n \varphi \rangle \\ &= \int_0^{\hat{T}} (K_n \rho_\lambda - g_n(T)) \int_0^T L_n(s,T) \varphi(s) ds dT \\ &= \int_0^{\hat{T}} \varphi(s) \int_s^{\hat{T}} (K_n \rho_\lambda - g_n(T)) L_n(s,T) dT ds \\ &= \int_0^{\hat{T}} \varphi(s) \left( \int_0^{\hat{T}} \tilde{L}_n(s,t) \rho_\lambda(t) dt - \int_s^{\hat{T}} g_n(T) L_n(s,T) dT \right) ds \\ &= \langle H_n \rho_\lambda, \varphi \rangle, \end{aligned} \quad (45)$$

we have

$$\langle \sum_{n=0}^k H_n \rho_\lambda + \lambda_1 \rho_\lambda - \lambda_2 \rho''_\lambda, \varphi \rangle = 0. \quad (46)$$

As the arbitrariness of  $\varphi$ , we can get the Euler equation as following

$$\sum_{n=0}^k H_n \rho_\lambda + \lambda_1 \rho_\lambda - \lambda_2 \rho''_\lambda = 0,$$

which is the necessary condition  $\rho_\lambda$  satisfies.

## 4. Numerical Experiments

In this section, we discuss the implementation for the calibration problem, present two numerical examples to illustrate the effectiveness of the proposed method, and examine the dependence of the calibration results on all the parameters  $k$ ,  $\lambda$  and the noise level  $\delta$ .

### 4.1. Discrete Scheme

Suppose the market prices of zero-coupon bond with maturity dates  $0 = T_0 < T_1 < T_2 < \dots < T_N = \hat{T}$  are given. Without loss of generality, we assume the dates are equal

distance distribution with  $\Delta T = \hat{T} / N$ . In addition, suppose that when  $T = T_0$ ,  $\rho(t) = \rho_0$ , when  $T_{i-1} < T \leq T_i (1 \leq i \leq N)$ ,  $\rho(t) = \rho_i$ .

Define Root Mean Square Error (RMSE) as follows

$$RMSE = \sqrt{\frac{1}{N} \sum_{i=1}^N (\rho(T_i) - \rho_i)^2}, \tag{47}$$

where  $\rho(T_i)$  is the exact solution and  $\rho_i$  is the numerical solution.

Based on midpoint discrete scheme, as  $s = T_i (i = 1, 2, \dots, N - 1)$ , The two integral equations in the right side of (40) can be discretized respectively as following

$$\begin{aligned} \int_0^{\hat{T}} \tilde{L}_n(T_i, t) \rho(t) dt &\approx \sum_{j=0}^{N-1} \int_{T_j}^{T_{j+1}} \tilde{L}_n(T_i, t) \rho(t) dt \\ &\approx \sum_{j=0}^{N-1} \tilde{L}_n(T_i, T_{j+\frac{1}{2}}) \frac{\rho_j + \rho_{j+1}}{2} \Delta T, \end{aligned} \tag{48}$$

where  $T_{j+\frac{1}{2}} = T_j + \frac{\Delta T}{2}$ .

$$\begin{aligned} \int_{T_i}^{\hat{T}} g_n(T) L_n(T_i, T) dT &\approx \sum_{j=i}^{N-1} \int_{T_j}^{T_{j+1}} g_n(T) L_n(T_i, T) dT \\ &\approx \sum_{j=i}^{N-1} \frac{g_n(T_j) + g_n(T_{j+1})}{2} L_n(T_i, T_{j+\frac{1}{2}}) \Delta T. \end{aligned} \tag{49}$$

In addition, the third term in the left side of the equation (39) can be discretized as

$$\rho_i'' = \frac{\rho_{i+1} - 2\rho_i + \rho_{i-1}}{\Delta T^2}. \tag{50}$$

Above all, we obtain

$$\begin{aligned} \sum_{n=0}^k \sum_{j=0}^{N-1} \tilde{L}_n(T_i, T_{j+\frac{1}{2}}) \frac{\rho_j + \rho_{j+1}}{2} \Delta T + \lambda_1 \rho_i \\ - \lambda_2 \frac{\rho_{i+1} - 2\rho_i + \rho_{i-1}}{\Delta T^2} = F_i, \quad i = 1, 2, \dots, N - 1. \end{aligned} \tag{51}$$

where

$$F_i = \sum_{n=0}^k \sum_{j=i}^{N-1} \frac{g_n(T_j) + g_n(T_{j+1})}{2} L_n(T_i, T_{j+\frac{1}{2}}) \Delta T. \tag{52}$$

The initial and boundary conditions in the equation (27) imply that

$$\rho_0 = \rho_1, \rho_{N-1} = \rho_N. \tag{53}$$

In order to further simplify the symbols, we introduce the notation  $l_{i,j}^n (i = 1, 2, \dots, N - 1)$  as follows

$$l_{i,j}^n = \begin{cases} (\tilde{L}_n(T_i, T_{\frac{1}{2}}) + \frac{1}{2} \tilde{L}_n(T_i, T_{1+\frac{1}{2}})) \Delta T, & j = 1, \\ \frac{\Delta T}{2} (\tilde{L}_n(T_i, T_{j-\frac{1}{2}}) + \tilde{L}_n(T_i, T_{j+\frac{1}{2}})), & j = 2, \dots, N - 1, \\ \frac{\Delta T}{2} \tilde{L}_n(T_i, T_{N-\frac{1}{2}}), & j = N. \end{cases} \tag{54}$$

Therefore

$$\left( \sum_{n=0}^k A_n + \lambda_1 E - \lambda_2 B \right) \rho = F, \tag{55}$$

where  $E$  is an identity matrix of  $N \times N$ ,

$$A_n = \begin{pmatrix} l_{1,1}^n & l_{1,2}^n & \dots & l_{1,N-1}^n & l_{1,N}^n \\ l_{2,1}^n & l_{2,2}^n & & l_{2,N-1}^n & l_{2,N}^n \\ \vdots & \vdots & \ddots & \vdots & \\ l_{N-1,1}^n & l_{N-1,2}^n & & l_{N-1,N-1}^n & l_{N-1,N}^n \\ 0 & 0 & \dots & -1 & 1 \end{pmatrix}_{N \times N},$$

$$B = \frac{1}{\Delta T^2} \begin{pmatrix} -1 & 1 & & & \\ 1 & -2 & 1 & & \\ & & \ddots & & \\ & & & 1 & -2 & 1 \\ & & & & -1 & 1 \end{pmatrix}_{N \times N}, F = \begin{pmatrix} F_1 \\ F_2 \\ \vdots \\ F_{N-1} \\ 0 \end{pmatrix},$$

### 4.2. Numerical Results

In the following, we give two examples for the calibration of implied volatility and consider the dependence of the numerical results on the parameters:  $k$ ,  $\lambda$  and the noise level  $\delta$ .

Example 1. We assume  $a = 0.05$ ,  $r_0 = 0.03$ ,  $\theta(t) = 0.1te^{-0.5t}$ ,

$$\hat{T} = 5, N = 10, \quad \rho(t) = \sigma^2(t) = 0.06 - 0.002 \left( -\frac{t^3}{3} + \frac{5t^2}{2} \right).$$

The market prices for zero-coupon bonds with different maturities are calculated by the equation (7).

Table 1. RMSE for different  $k$  and  $\lambda$ .

$\lambda^*$	$5e-3$	$1e-2$	$5e-2$	$1e-1$
$k = 0$	0.0037	0.0046	0.0067	0.0077
$k = 1$	0.0020	0.0020	0.0032	0.0040
$k = 2$	0.0018	0.0018	0.0016	0.0016
$k = 3$	0.0017	0.0015	0.0014	0.0013

Table 2. Minimum RMSE and the corresponding  $\lambda$ .

	$k = 0$	$k = 1$	$k = 2$	$k = 3$
$\lambda_1$	0.0038	0.0309	0.2308	0.9362
$\lambda_2$	0.0020	0.0174	0.1392	0.6538
RMSE	0.0011	9.4123e-4	8.1878e-4	7.9297e-4

First we consider the parameter  $k$  and assume that  $\lambda^* = \lambda_1 = \lambda_2$ . Let  $\lambda^* = 5e-3, 1e-2, 5e-2, 1e-1$  and  $k = 0, 1, 2, 3$ . Figure 1a-1d show the calibration results with different  $k$  and  $\lambda^*$ . Table 1 shows the corresponding RMSE. From Figure 1a-1d, it is clear that when  $\lambda^*$  is the same, a larger  $k$  gives better calibration results, which can be seen obviously from Table 1. That is easy to be understood from the expression (26) of regularization problem. In addition, from Figure 1a-1d we can also find that the error of the numerical solution at the end point is relatively large, which is due to that the kernel function  $L_n(T, T) = 0$ . But as the variable  $k$  gets larger, the error at the end point is well improved.

Next we consider the regularization parameters

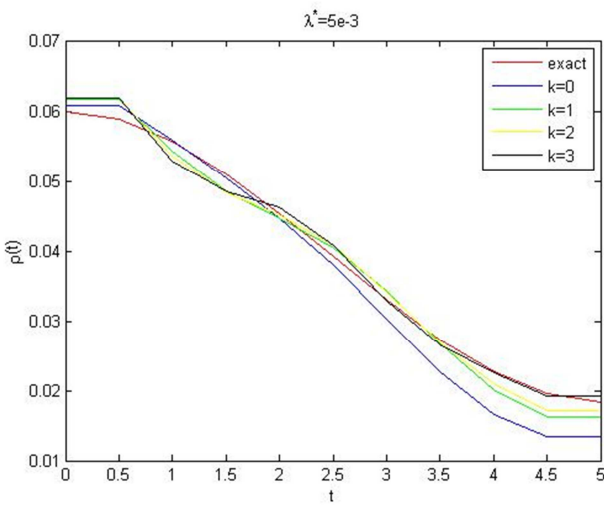


Figure 1a. Calibration results for different  $k$  and  $\lambda$ .

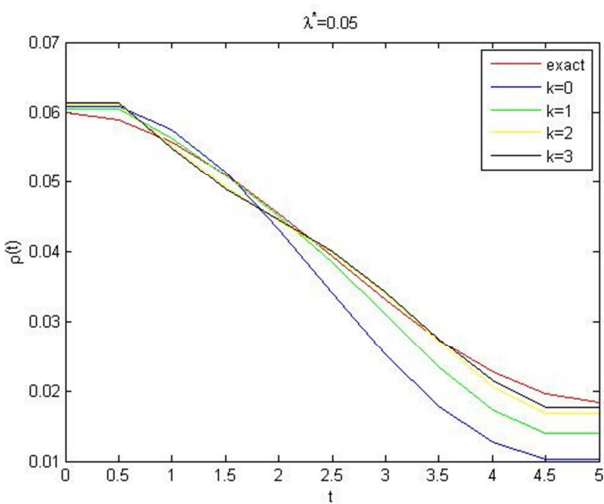


Figure 1b. Calibration results for different  $k$  and  $\lambda$ .

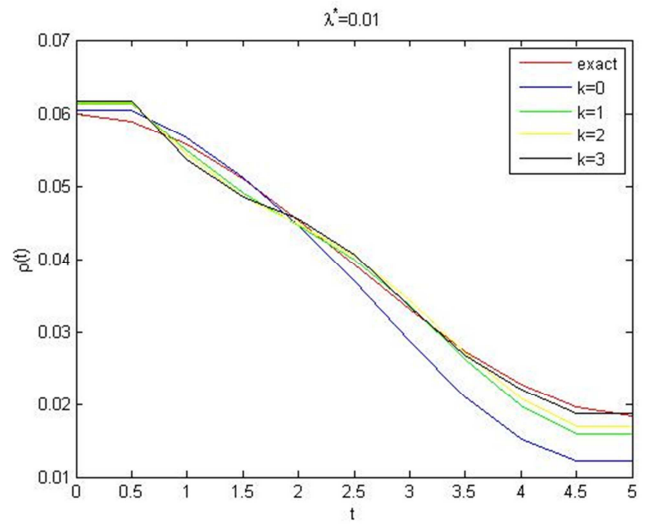


Figure 1c. Calibration results for different  $k$  and  $\lambda$ .

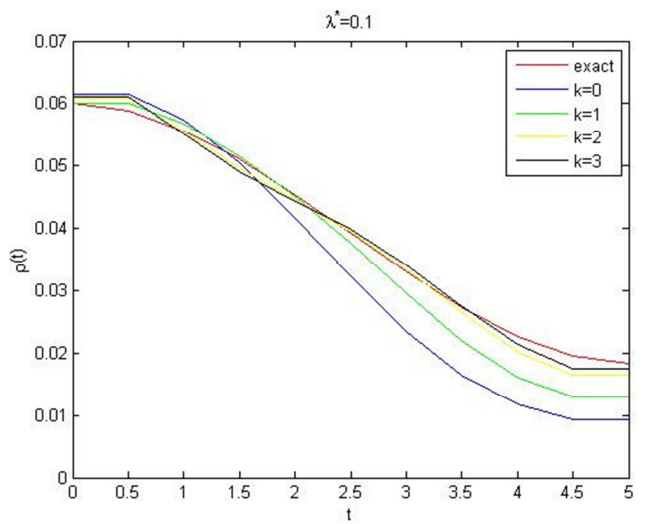


Figure 1d. Calibration results for different  $k$  and  $\lambda$ .

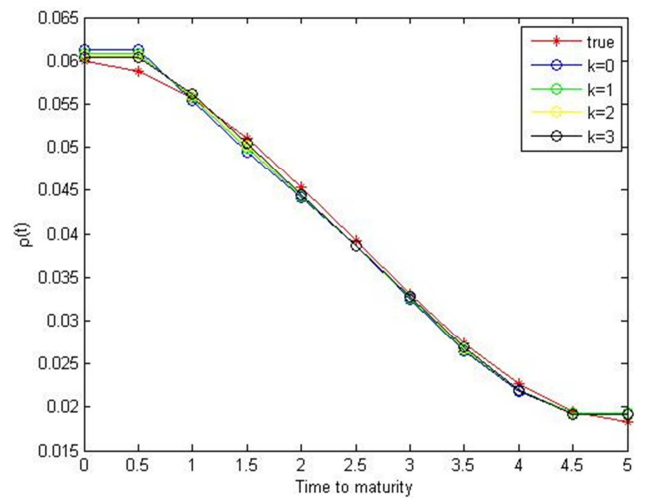


Figure 2. Exact and calibrated volatilities.

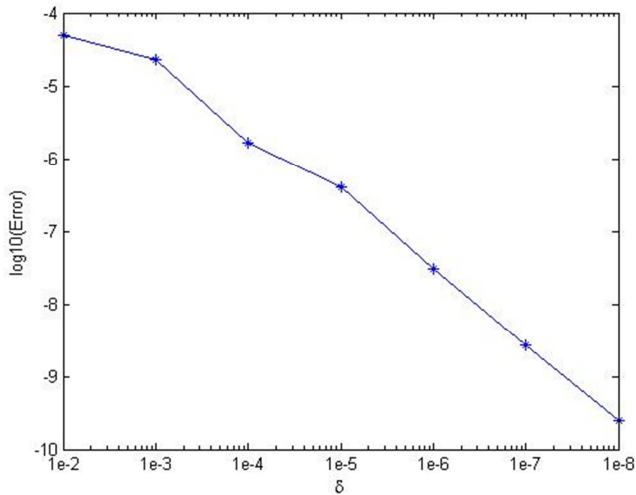


Figure 3. Error for different  $\delta$ .

$\lambda = (\lambda_1, \lambda_2)$ . From Table 1, we can see that for different  $k$ , the values of  $\lambda$  corresponding to minimum RMSE are different. Here we use the linear search method to choose the values of  $\lambda = (\lambda_1, \lambda_2)$ . Table 2 shows the minimum RMSE and the corresponding  $\lambda$  for different  $k$  which can further verify that larger  $k$  yields better calibration. Figure 2 shows the comparison of the corresponding numerical solution and the exact solution for different  $k$ .

Finally we consider the noise level parameter  $\delta$ . In the following we fix  $k = 3$ ,  $\lambda = (\lambda_1, \lambda_2) = (0.9362, 0.6538)$ .

Suppose that the noisy data takes the form

$$g_n^\delta(T) = g_n(T)(1 + \delta z), \tag{56}$$

where  $z$  stands for uniformly distributed random numbers.

Then we describe the influence of the noisy data to the numerical results by the following expression

$$Error = \sqrt{\frac{1}{N} \sum_{i=1}^N (\rho_i^\delta - \rho_i)^2}, \tag{57}$$

where  $\rho_i^\delta, \rho_i$  are respectively the numerical solutions with and without noisy data.

Figure 3 plots the corresponding RMSE with different noise levels  $\delta$ . It can be seen that smaller noise levels yield smaller RMSE and better calibration results which means that the numerical result is stable and our proposed method is feasible.

Example 2. Let  $\rho(t) = \sigma^2(t) = 0.01 \cos(\frac{\pi}{5}t) + 0.06$ , and the other variables are the same as those for example 1.

Again, we consider the three parameters which are the same as those in the first example. Considering the parameter  $k$ , table 3 gives the RMSE for different  $k$  and  $\lambda^*$ . Similarly, it can be seen that a larger  $k$  is needed in order to achieve better calibration for the same  $\lambda_1$  and  $\lambda_2$ .

Table 3. RMSE for different  $k$  and  $\lambda$ .

$\lambda^*$	$5e-3$	$1e-2$	$5e-2$	$1e-1$
$k = 0$	0.0151	0.0171	0.0209	0.0227
$k = 1$	0.0092	0.0101	0.0138	0.0157
$k = 2$	0.0053	0.0062	0.0080	0.0090
$k = 3$	0.0023	0.0027	0.0043	0.0051

Considering the parameter  $\lambda$ , table 4 gives the minimum RMSE and the corresponding  $\lambda$  for different  $k$ . In addition, the numerical solutions are plotted against exact solution with different parameters of  $k$  in Figure 4.

Table 4. Minimum RMSE and the corresponding  $\lambda$ .

	$k = 0$	$k = 1$	$k = 2$	$k = 3$
$\lambda_1$	0.0091	0.0785	0.6030	0.9940
$\lambda_2$	$8.65e-4$	0.0078	0.0630	0.1420
RMSE	0.0010	$8.4053e-4$	$7.0756e-4$	$6.9624e-4$

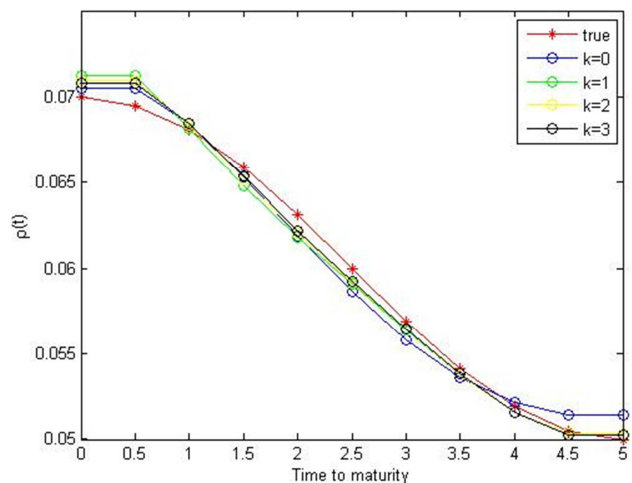


Figure 4. Exact and calibrated volatilities.

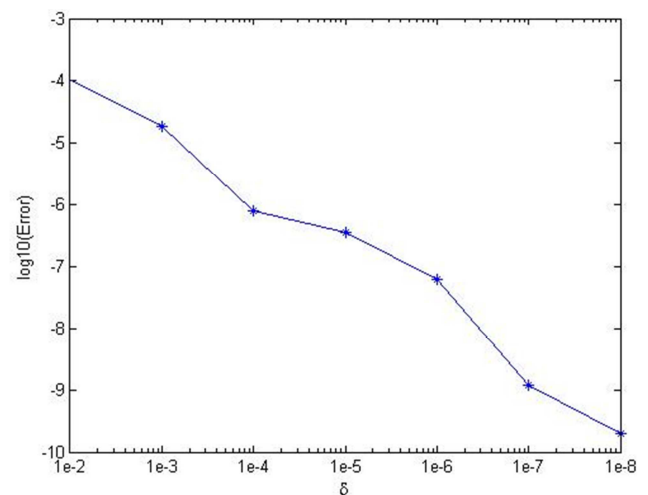


Figure 5. Error for different  $\delta$ .

Finally, in order to consider the parameter  $\delta$ , the other two parameters are fixed as  $k = 3$ ,  $\lambda = (\lambda_1, \lambda_2) = (0.9940, 0.1420)$ . Figure 5 shows the corresponding error for different  $\delta$  from

which we can see that smaller  $\delta$  contributes to a better calibration.

In conclusion, the results and conclusions obtained from example 2 are the same as those for the first example, which further verify that the proposed method is feasible.

Based on all of the above observation, it can be concluded that a larger parameter of  $k$  is preferred in order to obtain a better calibration.

## 5. Conclusion

In this paper, we present a stable and effective method for the calibration of the implied volatility in generalized Hull-White model from the market prices of zero-coupon bonds with different maturities. Based on the generalized Hull-White model, we transform the calibration problem to the regularization problem and establish the existence, stability of the solution and necessary condition that the solution satisfies. In the numerical experiment, two examples are considered and the effects of all the parameters are reported on the calibration. The results show that larger  $k$  yields better calibration and the proposed method is stable and effective. We point out some future directions along the line of calibration of parameters in interest rate models. It is interesting and challenging to solve the problem using the real market data. An even more challenging problem is to consider a calibration problem of two or even more parameters at the same time in the model, such as the drift term and the volatility term. We hope to be able to address these issues and report the progress elsewhere in the future.

## Acknowledgements

This work was supported by National Natural Science Foundation of China (11171349, 11571365, 11526123) and the Natural Science Foundation of Shandong Province (ZR2015PA010).

## References

- [1] O. Vasicek, An equilibrium characterization of the term structure, *Journal of Financial Economics*, 1977, 5(2): 177-188.
- [2] J. C. Cox, J. E. Ingersoll, S. A. Ross, A Theory of the Term Structure of Interest Rates, *Econometrica*, 1985, 53(2): 385-407.
- [3] J. Hull, A. White, Pricing Interest-Rate-Derivative Securities, *The Review of Financial Studies*, 1990, 3(4): 573-392.
- [4] K. R. Chan, G. A. Karolyi, F. Longstaff, A. B. Sanders, An Empirical Comparison of Alternative Models of the Short-Term Interest Rate, *Journal of Finance*, 1992, 47(3): 1209-1228.
- [5] J. Hull, A. White, Numerical Procedures for Implementing Term Structure Models I: Single-Factor Models, *Journal of Derivatives*, 1994, 2(1): 7-16.
- [6] J. Hull, A. White, The general Hull-White model and super calibration, *Finance Analysts Journal*, 2001, 57(6): 34-43.
- [7] I. Bouchoev, V. Isakov, N. Valdivia, Recovery of volatility coefficient by linearization, *Quantitative Finance*, 2002, 2: 257-263.
- [8] I. Bouchoev, V. Isakov, Uniqueness, stability and numerical methods for the inverse problem that arises in financial markets, *Inverse Problems*, 1999, 15(3): 95-116.
- [9] H. Egger, T. Hein, B. Hofmann, On decoupling of volatility smile and term structure in inverse option pricing, *Inverse Problem*, 2006, 22(4): 1247-1259.
- [10] R. Kramer, M. Richter, Ill-posedness versus ill-conditioning -an example from inverse option pricing, *Applicable Analysis*, 2008, 87(4): 465-477.
- [11] J. Hull, A. White, A generalized procedure for building trees for the short rate and its application to determining market implied volatility functions, *Quantitative Finance*, 2015, 15(3): 443-454.
- [12] A. M. Ferreira, J. A. García-Rodríguez, J. G. López-Salas, C. Vázquez, SABR/LIBOR market models: Pricing and calibration for some interest rate derivatives, *Applied Mathematics and Computation*, 2014, 242: 65-89.
- [13] Y. F. Wang, *Computational Methods for Inverse Problems and Their Applications*, Higher Education Press, Beijing, 2007. (In chinese)
- [14] H. Egger, H. W. Engl, Tikhonov regularization applied to the inverse problem of option pricing: convergence analysis and rates, *Inverse Problems*, 2005, 21(3): 1027-1045.
- [15] S. Doi, Y. Ota, An application of microlocal analysis to an inverse problem arising from financial markets, arXiv: 1404.7018, 2014.
- [16] C. Y. Tang, S. X. Chen, Parameter estimation and bias Correction for diffusion processes, *Journal of Econometrics*, 2009, 149(1): 65-81.
- [17] M. Rainer, Calibration of stochastic models for interest rate derivatives, *Optimization*, 2009, 58(3): 373-388.
- [18] M. Rodrigo, R. Mamon, An alternative approach to the calibration of the Vasicek and CIR interest rate models via generating functions, *Quantitative Finance*, 2014, 14(11): 1961-1970.
- [19] D. Duffie, R. A. Kan, Yield-factor model of interest rates, *Mathematical Finance*, 1996, 6(4): 379-406.